https://ntrs.nasa.gov/search.jsp?R=19740011343 2020-03-17T14:32:01+00:00Z

N74-19456

20. Cosmic Dust in the Atmosphere and in the Interplanetary Space at 1 AU Today and in the Early Solar System

H. FECHTIG
Max-Planck-Institut für Kernphysik
Heidelberg, Germany

Reliable measurements of cosmic dust abundances have been obtained by ionization detectors during particle impact and by collectors controlled either by inflight shadowing or by penetration-hole identification. A description of the techniques used is given.

Crater-number densities observed on the lunar surface and on lunar samples represent an important source of information on cosmic dust fluxes. The related results from the Apollo 11 and 12 missions are reviewed. The overall knowledge gained from these measurements leads to the following flux model: The cumulative flux Φ *vs mass* m *follows the extrapolation from larger meteoroid-size range (Watson's Law) and can be described by*

$$\Phi = 10^{-14.6} m^{-1} \qquad [m^{-2}\ s^{-1}]$$

The Pioneer 8 dust experiment and lunar samples indicate a depletion of the flux at approximately 10^{-8} *g. However, cosmic dust particles exist in interplanetary space at least down to 0.3* μ *diameter. They are interpreted as nonmetallic particles in the solar system.*

The atmosphere shows an enhancement in particles of about one order of magnitude compared to the flux in interplanetary space at 1 AU. No depletion or cutoff could be detected. These particles are interpreted as lunar debris or as disintegrated products from fireballs.

The numbers of large lunar craters (>140 m diameter) in Mare Tranquillitatis and in Oceanus Procellarum are compared with the meteoroid flux. These comparisons lead to a time-variable flux of $\Phi \cdot e^{-Bt}$, *with* $B = 2.6$ *and* $t =$ *time in* 10^9 *yr. Thus, the meteoroid flux at the formation of the lunar maria was approximately 4 orders of magnitude higher than today.*

THE RESULTS OF COSMIC DUST RESEARCH are reviewed in this paper. A description of a detector based on ionization during particle impact and of a controlled collection technique is given. Meteoroid fluxes today and in the early solar system are formulated from the distribution of craters in various areas of the Moon. Finally, the fluxes in interplanetary space, near the Earth, and in the upper atmosphere are discussed.

DETECTORS AND COLLECTORS

Experience has shown that detectors based on ionization during particle impact can achieve reliable results. Figure 1 shows a schematic diagram of the detector designed for the HEOS A2 satellite (Hoffmann, 1971). A particle hitting the hemispherical gold or tungsten target produces a plasma cloud during impact around the impact

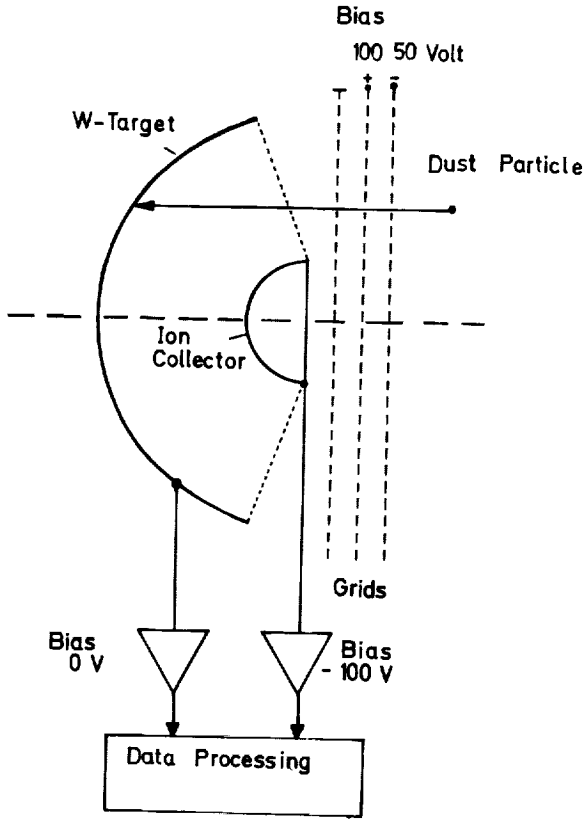

FIGURE 1.—HEOS dust-detector schematic diagram.

point. This plasma cloud expands radially. A concentrically mounted and negatively biased ion collector records the ions from this plasma cloud as the electrons are collected at the hemisphere. From one impact, the hemispherical target and ion collector sense pulses that are identical in pulse height, but different in polarity. From these coincident pulses one can derive mass and velocity of the impacted particle.

Figure 2 shows schematically the detector for the Helios probe (Grün, 1970). The target consists of inclined strips of gold or tungsten. Electrically biased grids in front of and behind the target separate the electrons and positive ions and produce coincident pulses on the grids. The ions are accelerated into a time-of-flight tube. At the end of the tube the ions are recorded as a function of flight time using a particle multiplier. Thus, a mass spectrum of the ion pulse is obtained. From these measurements information concerning chemical composition of the projectiles can be determined.

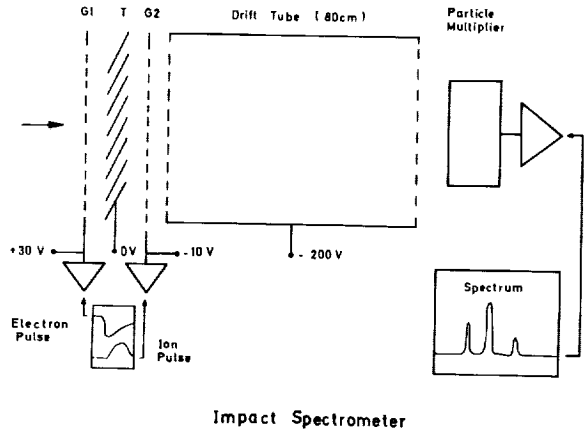

FIGURE 2.—Helios dust-detector schematic diagram.

These detectors have been calibrated using a 2-MV high voltage Van de Graaff electrostatic accelerator. Figure 3 shows the calibration of the detector in the mass range between 10^{-14} and 10^{-9} g for iron, aluminum, and carbon projectiles in the velocity range between 1 and 40 km/s (Hoffmann, 1971). For these ranges of measurements the following relationship holds:

$$C \sim m \cdot v^{3.5} \qquad (1)$$

where C = charge-pulse height
m = projectile mass
v = impact velocity

As shown by Auer and Sitte (1968), Grün (1970), and Hoffmann (1971), the rise time of the charge pulse—a function of the expansion velocity of the plasma—depends on the impact velocity of the projectile, i.e., on the plasma temperature. In figure 3 the rise time of the charge pulse is plotted as a function of impact velocity. Further experiments showed that rise time is independent of projectile mass.

Thus, particle mass m and impact velocity v can be determined from the knowledge of pulse height and rise time of the ion or electron pulse.

Ions are produced according to the relationship expressed in equation (1), a function of the impact velocity. Not only the intensity of the ion pulse, but also the composition of the ion pulse, i.e., the mass spectrum, depend strongly on the impact velocity as shown by Friichtenicht (1964), Grün (1970), and Dietzel (1971). Figure 4 shows an example of the spectra for various impact veloci-

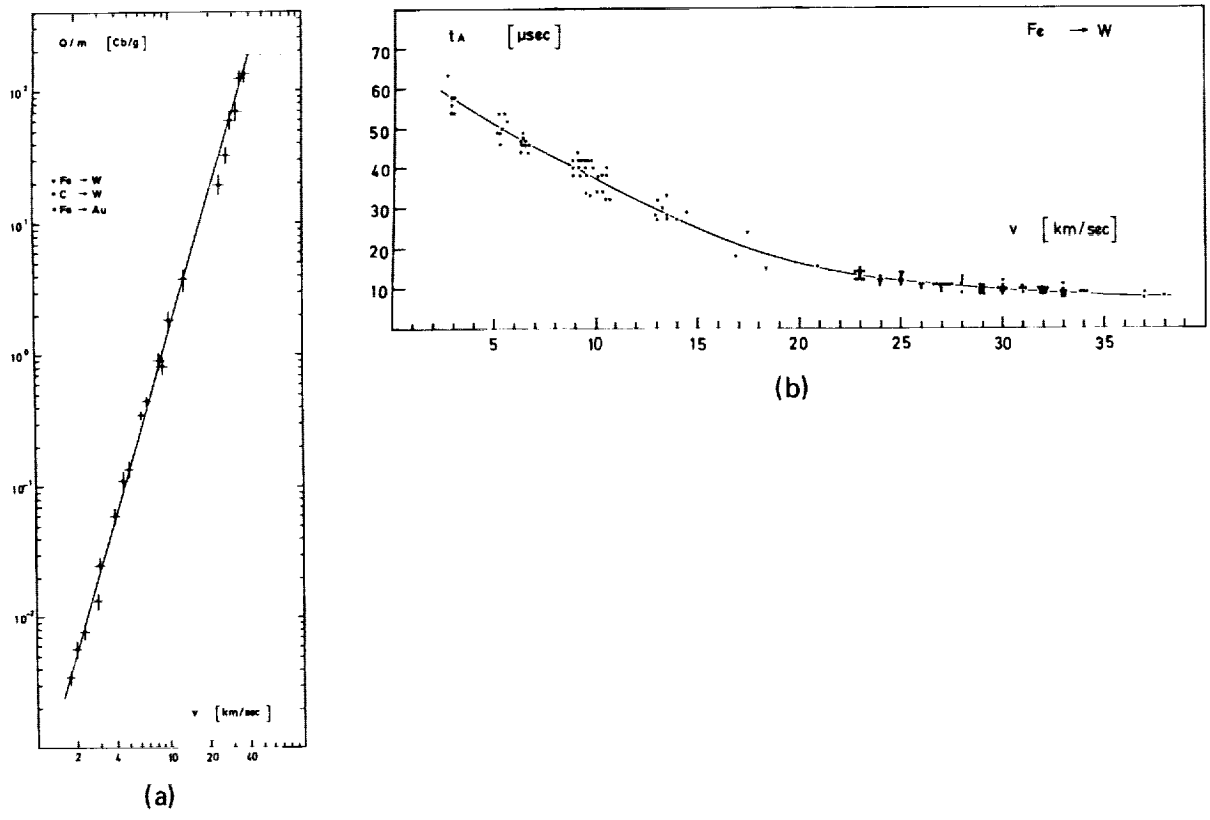

FIGURE 3.—Calibration characteristics of dust detectors. (a) Charge pulse per projectile mass vs impact velocity. (b) Rise time t_A vs impact velocity v.

ties of Al projectiles impacted on an Li-coated tungsten target. For low-impact velocities readily ionized alkalis can be detected that are present in the projectile or are impurities in the target material. Therefore, the Li ions are much more abundant than the Al ions because of different ionization potentials. At higher impact velocities (5 km/s) Al ions are as frequent as Li ions. At hypervelocity impacts (8 km/s) the Al line exceeds that of the Li line considerably (Dietzel, 1971).

The first version of the described detectors has been flown several times successfully aboard a rocket payload to detect cosmic dust in the upper atmosphere (Fechtig, Feuerstein, and Rauser, 1971; Rauser and Fechtig, 1972). Detectors based on the same technique are in Earth orbit on OGO III and in lunar orbit on Lunar Orbiter 35 (Alexander et al., 1971, 1972). Also, Berg and coworkers (Berg and Gerloff, 1971; Gerloff and Berg, 1971) have flown a similar detector aboard the Pioneer 8 and 9 deep-space probes. For the velocity measurements both groups use thin films in front of the detectors at the beginning of a time-of-flight tube. A first pulse is produced by a particle penetrating the film. The second pulse is obtained by particle impact on the solid target at the end of the time-of-flight tube. Thus, the impact velocity is measured. However, there may be undesired effects such as particle fragmentation (Grün and Rauser, 1969) during penetration or instrument cutoffs, especially for low-density projectiles at low relative impact-velocities.

The collectors of the first generation experiments (Hemenway and Soberman, 1962) applied the low-angle shadowing technique in the laboratory shortly before and after flight to mark contaminants by respective shadows. However, it appeared that the contamination problem was not solved by this technique. The last mounting

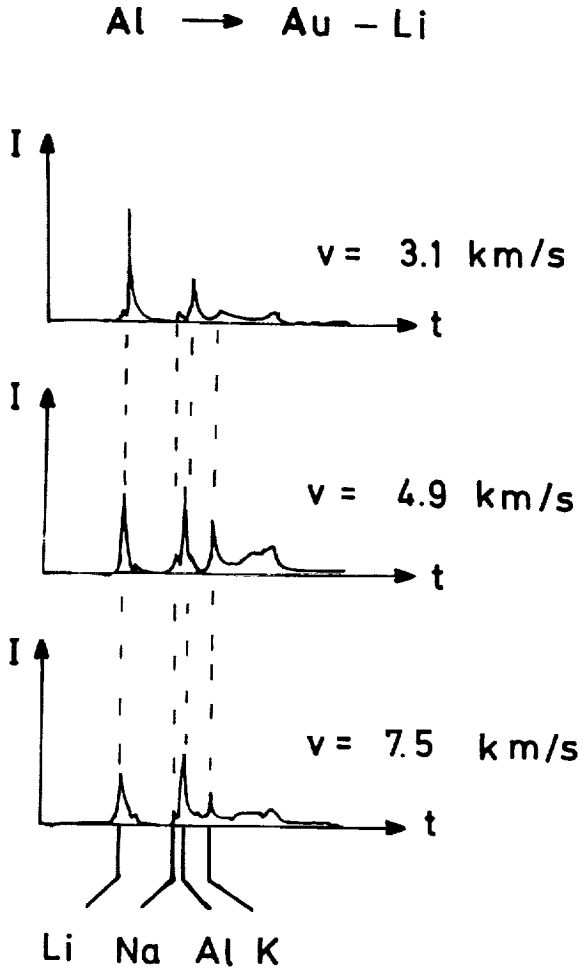

FIGURE 4.—Ion-pulse mass spectra. Projectiles: Al particles. Targets: Li-coated Au targets.

before flight and the first after flight were done before the correct shadows could identify the contaminants. For example, most round particles were produced by the evaporation process itself.

Recent collection experiments therefore apply an *in situ* shadowing technique, the so-called "inflight shadowing" (Skrivanek et al., 1970; Hemenway and Hallgren, 1970). By this technique the collection surface is shadowed several times during flight in different directions. Therefore, by different shadows one can discriminate in altitude and also exclude pre- and post-flight contaminants. Particles that may be produced by the inflight shadowing device can be identified chemically.

Another control technique is based on the penetration-hole identification first proposed by Yaniv and Shafir (1967), and, in another version, applied by our group (Auer et al., 1970): Particles must penetrate a thin nitrocellulose film before impacting on a solid target. Figure 5 shows the collector (metal plates) with a thin film mounted in front. Figure 5 also shows a penetration hole with a particle-strewn field beneath. The particle obviously was a low-density one that fragmentated as it penetrated the foil.

The inflight shadowing technique has the advantage of collecting very small particles (0.1-μ-diameter range) at low relative velocities. However, the collection area is comparatively small ($\sim$100 mm^2). The penetration-hole identification method is applicable for large surfaces ($\sim$100 cm^2), implying a cutoff because of limited penetrability of micron-sized particles at low relative velocities.

LUNAR CRATER DISTRIBUTIONS AND EARLY METEOROID FLUXES

The distribution of craters in various lunar areas is an important source of information concerning the distribution of meteoroids in the interplanetary space at 1 AU. Figure 6 shows the distribution of lunar impact craters as a function of crater diameters for the Mare Tranquillitatis (MT) and the Oceanus Procellarum (OP) as published by Shoemaker et al. (1970). The large craters on the production curve (>140 m diameter in MT and >50 m diameter in OP) follow a $D^{-2.9}$ distribution law which corresponds well with the overall m^{-1} distribution of the meteoroids (D = crater diameter, m = meteoroid mass). The deviation from -3 is explained by a variable D/d ratio of crater diameters to projectile diameters. Therefore, these crater numbers are considered as the time-integral of impacts since the existence of these lunar areas. Since MT is older than OP, MT has more large craters than OP. MT averages 2.4 times as many large craters as OP (Shoemaker et al., 1970), although MT is only 10 percent older than OP according to dating results of the related lunar samples (Albee et al., 1970).

A similar relation exists between the number of large craters in the Lunar Highlands compared to the related number in MT or OP. According to

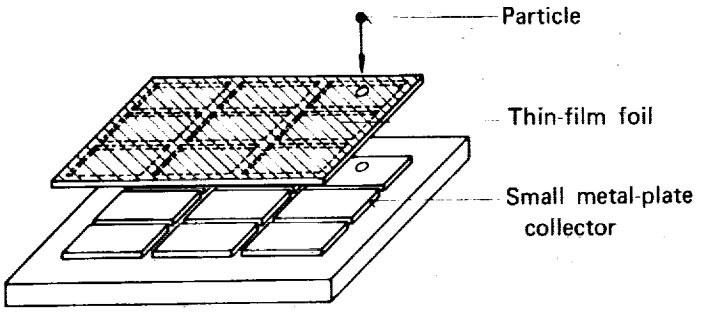

(a)

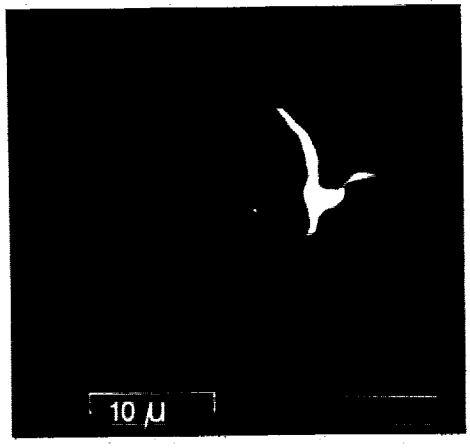

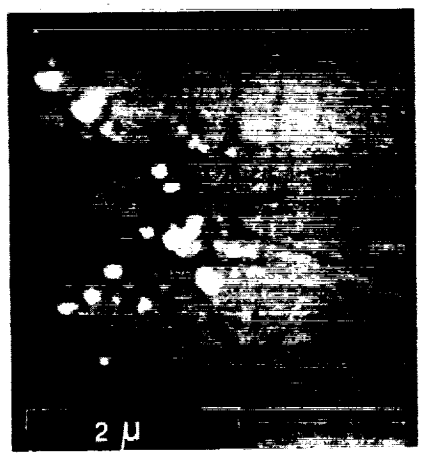

(b)

FIGURE 5.—(a) Controlled collector by hole identification. (b) Hole-fragmented particle.

Hartmann (1966) the number of large craters in the Southern Lunar Highland is as much as 30 to 50 times higher than in MT.

These crater-number densities cannot be interpreted on the basis of a time-constant meteoroid influx. Baldwin (1969, 1970, 1971) and Hartmann (1970) have plotted the crater-number densities of various maria as a function of age normalized by the known ages of MT and OP. We tried to combine these observations with meteoroid fluxes known from direct measurements (Bloch et al., 1971).

Let us first assume a general flux function $\varphi(m)$ in differential form or

$$\Phi(m) = \int_{m_0}^{\infty} \varphi(m)\, dm$$

in integral form known from direct observations. If one assumes that the decrease of meteoroids in the past is only given by impacts on planets and their moons, one can write:

$$-\frac{dN}{dt} \sim N \qquad (2)$$

Therefore, the time dependence is

$$N = N_0 e^{-Bt}$$

an exponential function. For the meteoroid flux in the past one can define a flux function $f(m, t)$ in differential form or $F(m, t)$ in integral form as follows:

$$\begin{aligned} f(m, t) &= \varphi(m) \cdot e^{-Bt} \\ F(m, t) &= \Phi(m) \cdot e^{-Bt} \end{aligned} \qquad (3)$$

For today $t=0$. The flux functions are $f(m, 0) = \varphi(m)$ and $F(m, 0) = \Phi(m)$. To determine B one can compare the numbers of craters in MT and OP in relation to the related ages:

$$\int_{-3.6}^{0} \int_{m_0}^{\infty} \varphi(m) \cdot e^{-Bt}\, dm\, dt = R \cdot \int_{-3.3}^{0} \int_{m_0}^{\infty} \varphi(m) \cdot e^{-Bt}\, dm\, dt \qquad (4)$$

with $R = 2.4$, the average ratio of large craters in MT to OP. From these determinations one finds

$$B = 2.6 \qquad (5)$$

The time variable flux function therefore reads:

$$\begin{aligned} f(m, t) &= \varphi(m) \cdot e^{-2.6t} \\ F(m, t) &= \Phi(m) \cdot e^{-2.6t} \end{aligned} \qquad (6)$$

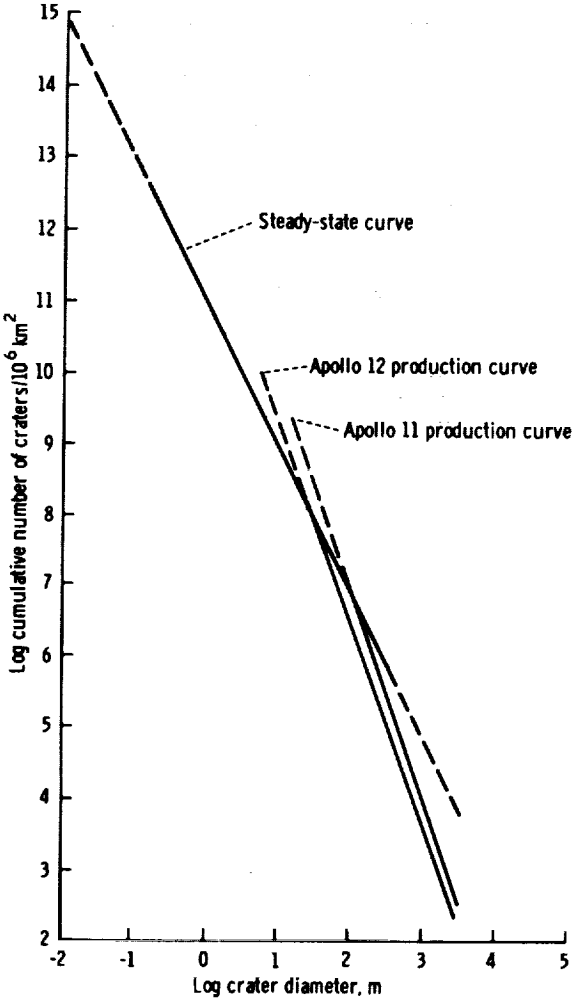

FIGURE 6.—Size frequency distribution of lunar craters at the Apollo 11 and 12 landing sites according to Shoemaker et al. (1970).

If one applies this formalism to the model age of the Lunar Highlands (LH) of $4.6 \cdot 10^9$ yr, the Lunar Highlands would show 12 times as many large craters as MT and therefore the production curve would begin at about 3-km diameter. Table 1 shows the enhancement of the meteoroid flux at the formation of MT, OP and LH by 4 to 5 orders of magnitude.

So far no special flux function $\Phi(m)$ for the present meteoroid flux has been used. Gault (1970) tried to compare the densities of large craters in MT with flux rates based on a time-constant influx. He used fluxes according to Naumann (1966) and Hawkins (1963) and according to Shoemaker (Gault, 1970). Gault's conclusion, assuming a time-constant influx, was consistent with the crater distributions in MT. However, a time-constant influx cannot explain crater distribution in the Lunar Highlands or explain the difference in distributions between MT and OP related to their absolute formation ages. But these can be explained if one accepts the flux to be

TABLE 1.—*Meteoroid Fluxes at the Formation of OP, MT, and LH*

Area	Age (10^9 *yr*)	$F(m, t)$
OP	3.3	$5.3 \times 10^3\ \Phi$
MT	3.65	$1.3 \times 10^4\ \Phi$
LH	4.6	$1.6 \times 10^5\ \Phi$

$$\Phi = 10^{-14.6}\, m^{-1} \qquad [m^{-2}\, s^{-1}] \qquad (7)$$

This flux function, equation (7), is lower than the one given by Naumann, Hawkins, and Shoemaker. But equation (7) does agree with the flux given by Watson (1956) and will be discussed in the next section of this paper with respect to other flux data.

If one accepts, for the moment, this flux function to be valid for today, the time-variable flux is

$$F(m, t) = 10^{-14.6} m^{-1} e^{-2.6t} \qquad (8)$$

The comparison with the crater-number densities in MT and OP works if one further accepts the D/d values for large craters to be on the order of 10. This value is quite low, but the corresponding value of 2 for μ-sized craters is experimentally known (Bloch et al., 1971; Mandeville and Vedder, 1971). This information suggests that the flux assumed is still too high for the large-crater range (km diameters). The fact that the meteoroids show a d^{-3} distribution and the craters show a $D^{-2.9}$ distribution is interpreted in the variability of the D/d values of 2 for μ-sized craters at 20 km/s impact velocity and increasing with increasing meteoroid diameters.

The distribution of smaller craters (<140 m diameter in MT and <50 m diameter in OP) in the diagram of figure 6 shows a D^{-2} distribution for MT and OP. As interpreted by Shoemaker

et al. (1970) and experimentally shown by Gault (1970), small craters are lacking because of meteoroid impacts (for example, from erosive effects of ejecta material), solar wind (from sputtering effects), and possibly thermal gradient influences. This distribution could be verified down to crater diameters of about 50 μ as shown by Hörz, Hartung, and Gault (1971) and by Neukum (1971).

The time-variable formalism can be applied to crater sizes in the equilibrium status and mean crater lifetimes t can be calculated by the formula

$$\Phi(m) \int_{-t}^{0} e^{-2.6t}\, dt = \frac{N}{F}$$

where

N/F = cumulative number of craters on the equilibrium curve

$\Phi(m)$ = cumulative flux of the corresponding meteoroids.

For 0.3 mm diameter craters (observable on small lunar surface samples) the mean crater lifetime is approximately 10^7 yr. For 1-m diameter craters the lifetime is 10^8 to 10^9 yr which is consistent with cosmic-ray-exposure age determinations for the Apollo 12 soil of 350 million yr (Kirsten, Steinbrunn, and Zähringer, 1971).

The latest progress has been gained by scanning smooth-crater glass linings of sample No. 12063.106, glass-coated sample No. 12024.8.1, and a glass ellipsoid from sample No. 14257 (Fechtig, Mehl, Neukum, and Schneider, 1972). It was possible to discover and count craters down to about 0.3μ diameters with a $D^{-0.8}$ size distribution. The crater number density for craters $\geq 1\mu$ diameter is found to be 10^3 craters per cm^2. The conversion into fluxes according to Neukum and Dietzel (1971) results in a $m^{-0.6}$ distribution down to 0.15μ diameter particles (fig. 7).

The overall meteoroid flux distribution as derived from the distribution of lunar craters is shown in the flux diagram of figure 8. The general slope in the mass distribution is -1 according to equation (7). The distribution shows a depletion at about 30μ-diameter particle size. There, the slope changes to -0.6 down to meteoroid masses of about 10^{-15} g. These submicron-sized craters are considered as an important observation concerning the existence of submicron-sized solid particles in the interplanetary space. The lower slope in the mass distribution may be interpreted by a variable cutoff for small particles due to the Poynting-Robertson effect. This variability is caused mainly by different eccentricities of the particle orbits (Dohnanyi, 1969) and a variability of the chemical composition of the particles. According to Shapiro et al. (1966) metallic particles show a much higher cross section for the influence of the solar electromagnetic interaction than nonconductive particles. Therefore, the smallest particles would be the nonmetallic particles since the metallic component cannot survive as close as 1 AU to the Sun.

THE PRESENT METEOROID FLUX

Figure 9 shows the flux of cosmic dust cumulatively plotted as a function of mass. The results are discussed in four groups:

(a) Results from lunar crater distributions

(b) Results obtained in interplanetary deep space (including zodiacal light measurements)

(c) Spacecraft results (between Earth and Moon and from Lunar Orbiter)

(d) Results from dust collectors and detectors in the atmosphere (rocket- and balloon-borne experiments).

Lunar Craters

The general mass distribution derived from lunar-crater statistics have been discussed in the previous section. The results are labeled "MOON" in figure 9. The slope for larger particles ($>30\mu$ diameter) is -1, for smaller particles ($<30\mu$ diameter), -0.6.

Interplanetary Deep Space

Measurements were reported by Alexander et al. (1971) from the Mariner IV dust experiment and by Berg and Gerloff (1971) from the Pioneer 8 and 9 experiments. Leinert (1971) has calculated fluxes from earlier zodiacal-light measurements by Elsässer (1958), Ingham (1961) and Weinberg (1964).

From the Pioneer dust experiment a cutoff was

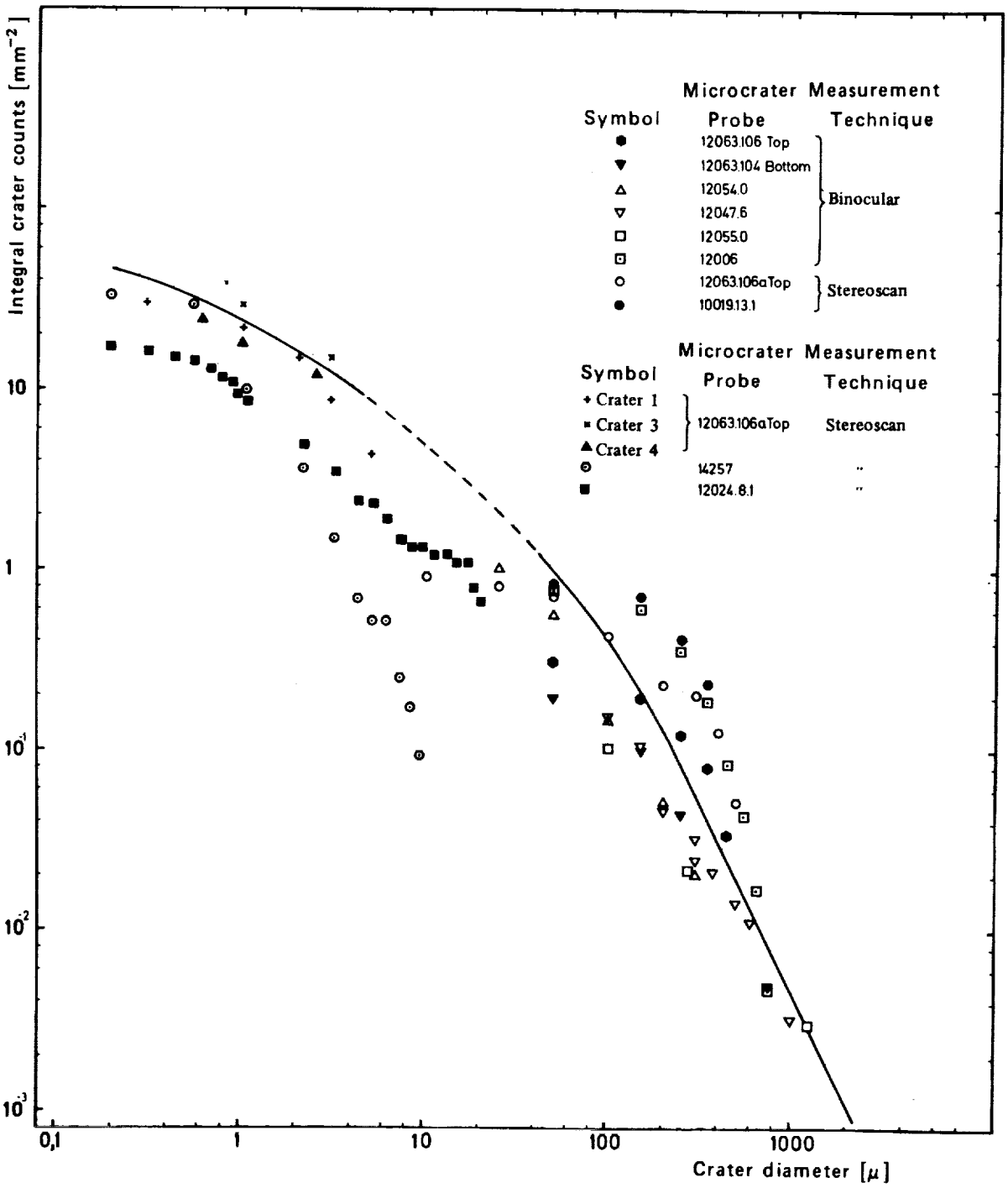

FIGURE 7.—Microcrater distribution on various lunar samples.

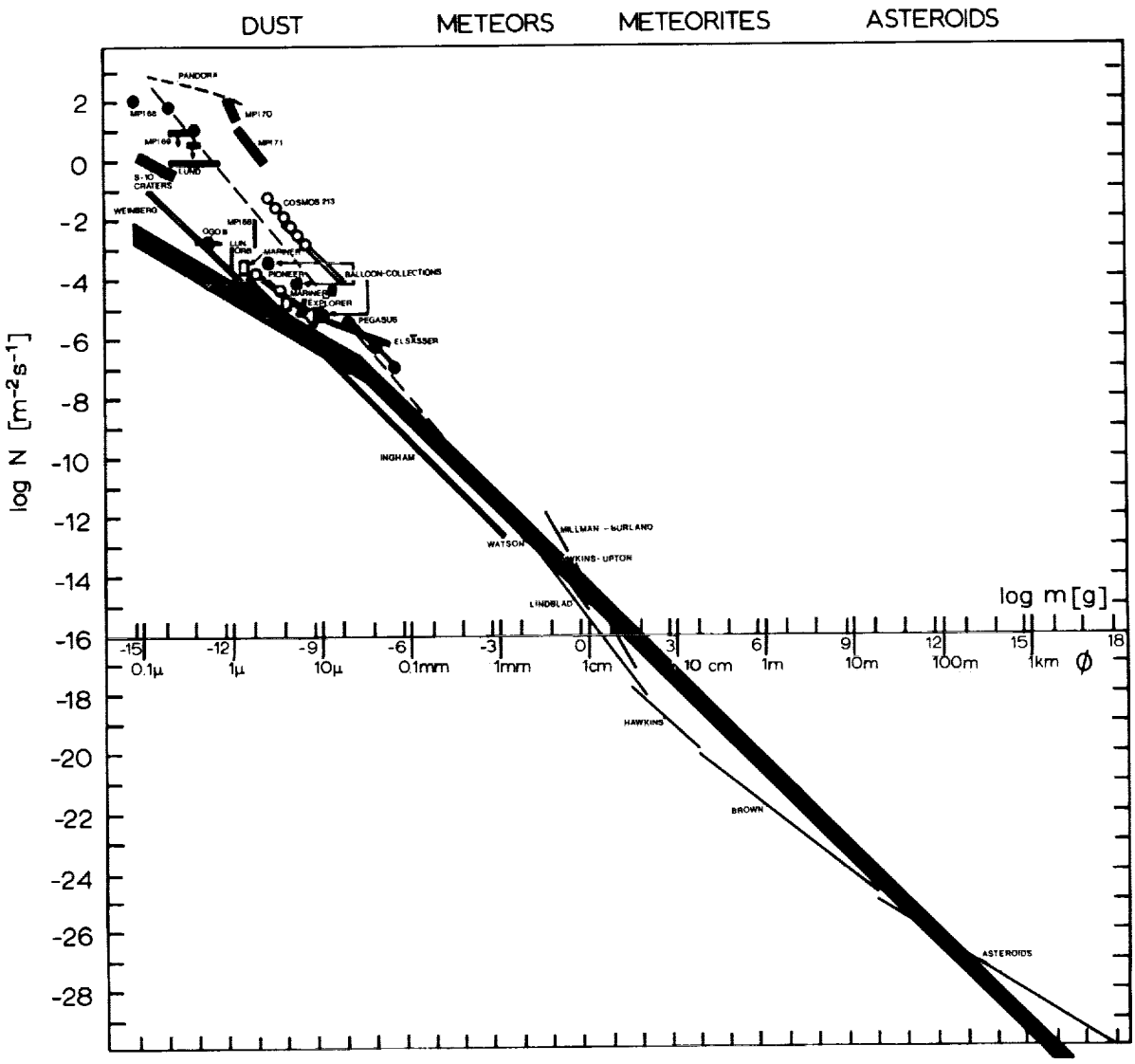

FIGURE 8.—Cumulative meteoroid fluxes as a function of mass.

reported (Berg and Gerloff, 1971; Gerloff and Berg, 1971) at about 10^{-11} g and interpreted with orbit elements according to Dohnanyi (1969). Generally, the *in situ* results and the indirect measurements of the zodiacal light are very similar. The cutoff from the zodiacal-light measurements is a question of interpretation.

A comparison of these results with the results from lunar-crater statistics leads one to question the Pioneer detection cutoff of particles at 10^{-11} g. On the contrary, submicron-sized lunar craters have been found, thus indicating the existence of submicron-sized particles in the interplanetary space. Two possible explanations of this apparent discrepancy are as follows:

(a) If a variable particle-size cutoff exists because of chemical composition, the smallest particles are nonmetallics (silicates, quartz). The general lack of metals for the smallest particles influences heavily the ion production of the impact detectors used in the Pioneer mission as discussed in a previous section of this paper.

(b) The Pioneer dust experiment with a quasi-circular orbit around the Sun cannot detect

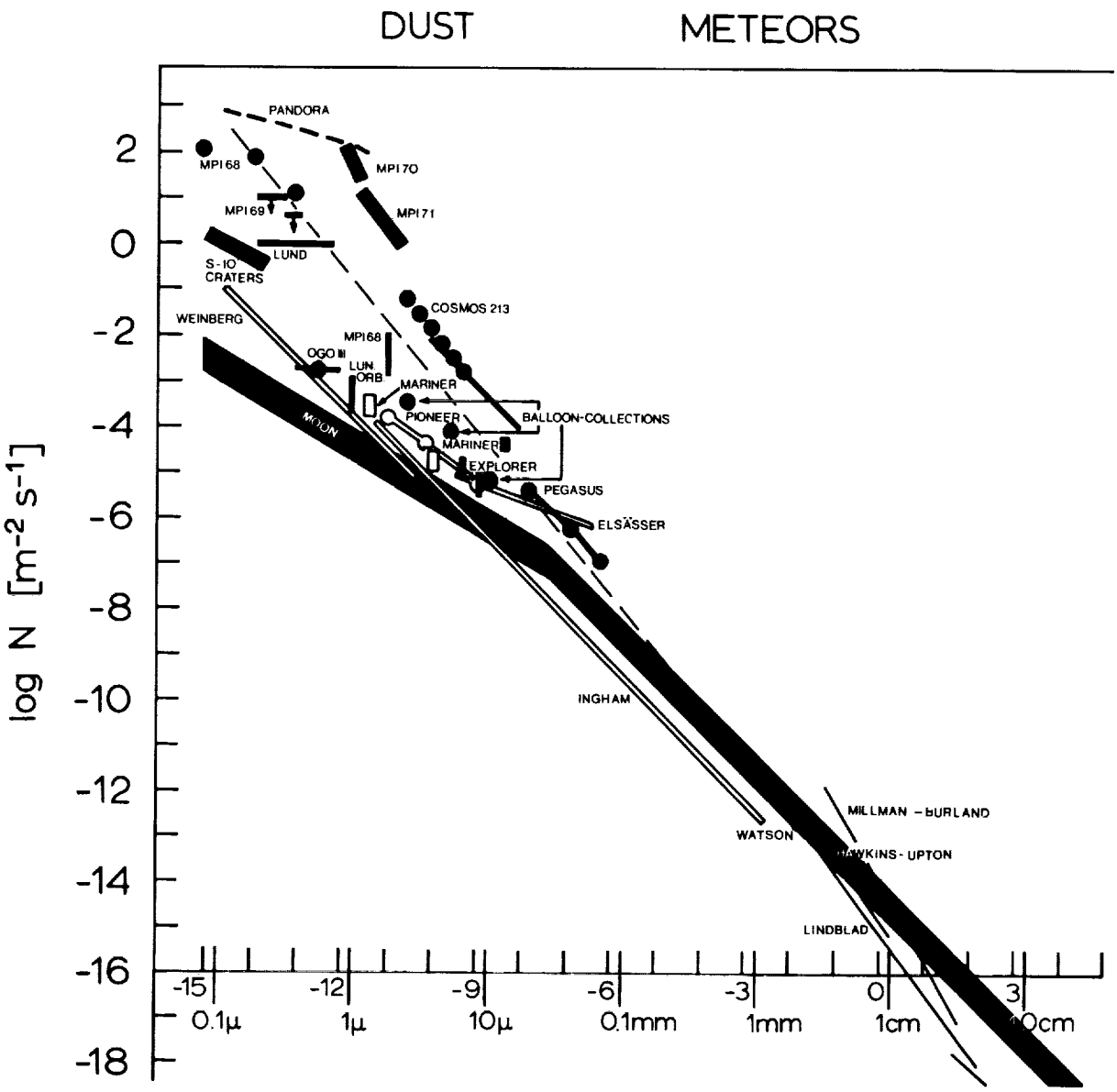

FIGURE 9.—Cumulative cosmic dust fluxes as a function of mass.

circularly orbiting particles, since the relative velocity is not high enough for small particles to penetrate the thin foil in front of the detector and produce enough ions to be recorded. (The lowest relative velocity must exceed 0.7 km/s to be detected.)

Spacecraft Results

Higher fluxes have been measured by Earth and Moon satellites. Using different techniques, results were reported from the following experiments: capacitive detectors on Pegasus (Anon., 1966, 1967), penetration-experiment on Explorer XXIII (Naumann, 1966), microphones on Cosmos 213 (Nazarova and Rybakov, 1971), ionization detector on OGO III (Alexander, Arthur, and Bohn, 1971), ionization detector on Lunar Orbiter 35 (Alexander et al., 1971), and the S 10- S 12-craters (Hemenway et al., 1968). Two possible explanations for these higher near-Earth fluxes are:

(a) Temporarily higher influxes of lunar debris are produced both by impacts of meteor streams and sporadic dust particles on the lunar surface. This origin was discussed by Alexander et al. (1971). Gault et al. (1963) and Colombo et al. (1966) have also discussed this problem.

(b) Fireballs that might be of low-density material (Dubin, 1971) form disintegrated products.

Atmospheric Dust

The highest flux numbers are reported from experiments in the atmosphere using rocket and balloon-borne dust collectors and detectors. Based on the Pandora and the balloon-top collections by Hemenway et al. (1971), the balloon collections of Brownlee et al. (1971), the MPI 68, 69, 70 collections (Auer et al., 1970; Fechtig and Feuerstein, 1970; Fechtig, Feuerstein, and Rauser, 1971), the LUSTER 68 flight through a NLC display (Farlow et al., 1970), and the detector results of "Lund" (Lindblad et al., 1970), MPI 70, 71 (Fechtig, Feuerstein, and Rauser, 1971; Rauser and Fechtig, 1972), one can state the following items:

(a) No cutoff down to masses of about 10^{-15} g could be found.

(b) Easily fragile particles are evident and support Jacchia's (1955) and Verniani's (1969) observations of low-density material.

(c) Large variations probably due to meteor shower activities and Noctilucent Cloud displays are observed for the fluxes.

(d) Still not sufficiently known is the influence of the upper atmosphere on the dynamics of small particles. In 1970 we (Rauser and Fechtig, 1972) measured a velocity profile of micron-sized particles between 70 and 110 km altitude.

The measured velocities are lower than expected at 110 km altitude which suggests that the particles are of a fluffy low-density material. However, the measured velocities are about 2 orders of magnitudes higher than expected (Kornblum, 1969) at 70 to 80 km altitudes. The existence of a temperature minimum at about 85 km altitude leads one to expect a diameter and/or density increase of particles by absorption of condensable material like water or CO_2. This mechanism might also explain the Noctilucent Clouds. A layering effect can be calculated from the detailed data.

Finally, total influx rates can be calculated from the flux curve. One calculates a total daily influx of interplanetary material on the Earth of about 25 tons. This number is consistent with investigations by Keays et al. (1970). These authors have investigated lunar samples for meteoritic components. Although the investigations were carried out in a completely different scientific field, the results show an agreement.

SUMMARY

This paper contains a description of techniques used in recent experiments to detect and analyze cosmic dust and micrometeorites. Furthermore, the results both from the study of lunar crater statistics and from *in situ* measurements have been reviewed.

Ionization detectors and controlled collectors represent important progress in the techniques used in the research field of cosmic dust.

The results from lunar crater statistics show an agreement with the results obtained from *in situ* measurements in interplanetary space and derived from zodiacal-light measurements. The near-Earth results show an enhancement in the flux numbers. This can be caused either by secondary lunar debris or by disintegration of low-density fireballs in the outer atmosphere.

For future experiments *in situ* measurements are needed in interplanetary space. The question of the chemical composition of particles is important with respect to the origin of cosmic dust.

REFERENCES

ANON., 1966. The meteoroid satellite project Pegasus, first summary report, *NASA Tech. Note* **D-3505**.

ANON., 1967. Scientific results of project Pegasus, interim report, *NASA* **X-53629**.

ALBEE, A. L., ET AL., 1970. Ages, irradiation history, and chemical composition of lunar rocks from the Sea of Tranquillity, *Science*, **167**, 463–466.

ALEXANDER, W. M., ARTHUR, C. W., AND BOHN, J. L., 1971. Lunar Explorer 35 and OGO III: dust particle measurements in selenocentric and cislunar space from 1967 to 1969, *Space Research XI*, 279–285.

ALEXANDER, W. M., ARTHUR, C. W., BOHN, J. L., JOHNSON, J. H., AND FARMER, B. J., 1972. Lunar Explorer 35: 1970 dust particle data and shower related picogram ejecta orbits, *Space Research XII*, 349–355.

AUER, S., FECHTIG, H., FEUERSTEIN, M., GERLOFF, U., RAUSER, P., WEIHRAUCH, J., AND LINDBLAD, B. A., 1970. Rocket experiments using extremely sensitive detectors for cosmic dust particles, *Space Research X*, 287–294.

AUER, S., AND SITTE, K., 1968. Detection technique for micrometeoroids using impact ionization, *Earth Planetary Sci. Letters*, **4**, 178–183.

BALDWIN, R. B., 1969. Absolute ages of the lunar maria and large craters, *Icarus*, **11**, 320–331.

——, 1970. Absolute ages of the lunar maria and large craters, II. The viscosity of the Moon's outer layers, *Icarus*, **13**, 215–225.

——, 1971. On the history of lunar impact cratering: the absolute time scale and the origin of planetesimals, *Icarus*, **14**, 36–52.

BERG, O. E., AND GERLOFF, U., 1971. More than two years of micrometeorite data from two Pioneer satellites, *Space Research XI*, 225–235.

BLOCH, M. R., FECHTIG, H., GENTNER, W., NEUKUM, G., AND SCHNEIDER, E., 1971. Meteorite impact craters, crater simulations and the meteoroid flux in the early solar system, *Proc. Second Lunar Sci. Conf., Geochim. Cosmochim. Acta, Suppl.*, **2**, 2639–2652.

BROWNLEE, D., HODGE, P., AND BUCHER, W., 1971. Extraterrestrial dust in the stratosphere, unpublished.

COLOMBO, G., SHAPIRO, I. I., AND LAUTMAN, D. A., 1966. The Earth's dust belt: fact or fiction? 3. Lunar ejecta, *J. Geophys. Res.*, **71**, 5719–5731.

DIETZEL, H., 1971. Univ. Heidelberg.

DOHNANYI, J. S., 1969. On the origin and distribution of Meteoroids, *Bellcomm. Inc.*, **TR 69-105-3-2**.

DUBIN, M., 1971. Introduction, presented at COSPAR Meeting, Seattle, 1971.

ELSÄSSER, H., 1958. Interplanetare materie, *Milt. Astr. Inst. Tübingen*, **35**, 73.

FARLOW, N. H., FERRY, G. V., AND BLANCHARD, M. B., 1970. Examination of surfaces exposed to a noctilucent cloud, August 1, 1968, *J. Geophys. Res.*, **75**, 6736–6750.

FECHTIG, H., AND FEUERSTEIN, M., 1970. Particle collection results from a rocket flight on August 1, 1968, *J. Geophys. Res.*, **75**, 6751–6757.

FECHTIG, H., FEUERSTEIN, M., AND RAUSER, P., 1971. Simultaneous collection and detection experiment for cosmic dust, *Space Research XI*, 335–346.

FECHTIG, H., MEHL, A., NEUKUM, G., AND SCHNEIDER, E., 1972. Meteoroid fluxes as derived from lunar crater number densities, unpublished.

FRIICHTENICHT, J. F., 1964. Micrometeoroid simulation using nuclear accelerator techniques, *Nucl. Instr. Methods*, **28**, 70–78.

GAULT, D. E., 1970. Saturation and equilibrium conditions for impact cratering on the lunar surface: criteria and implications, *Radio Sci.*, **5**, 273–291.

GAULT, D. E., SHOEMAKER, E. M., AND MOORE, H. J., 1963. Spray ejected from the lunar surface by meteoroid impact, *NASA Tech. Note* **D-1767**, Washington.

GERLOFF, U., AND BERG, O., 1971. A model for predicting the results of in situ meteoroid experiments: Pioneer 8 and 9 results and phenomenological evidence, *Space Research XI*, 397–413.

GRÜN, E., 1970. Massenspektrometrische Analysen von Ionen beim Aufschlag schneller Staubteilchen, thesis, Univ. Heidelberg.

GRÜN, E., AND RAUSER, P., 1969. Penetration studies of iron dust particles in thin foils, *Space Research IX*, 147–154.

HARTMANN, W. K., 1966. Martian cratering, *Commun. Lunar Planet. Lab.*, Univ. Ariz., **4**, part 4, No. 65, 121–131.

——, 1970. Lunar cratering chronology, *Icarus*, **13**, 299–301.

HAWKINS, G. S., 1963. Impacts on the Earth and Moon, *Nature*, **197**, 781.

HEMENWAY, C. L., AND HALLGREN, D. S., 1970. Time variation of the altitude distribution of the cosmic dust layer in the upper atmosphere, *Space Research X*, 272–280.

HEMENWAY, C. L., HALLGREN, D. S., AND KERRIDGE, J. F., 1968. Results from the Gemini S–10 and S–12 micrometeorite experiments, *Space Research VIII*, 521–535.

HEMENWAY, C. L., HALLGREN, D. S., LANDATE, A. T., PATASHNICK, H., RENZEMA, T. S., AND GRIFFITH, O. K., 1971. A new high altitude balloon-top cosmic dust collection technique, *Space Research XI*, 393–395.

HEMENWAY, C. L., AND SOBERMAN, R. K., 1962. Studies of micrometeorites obtained from a recoverable sounding rocket, *Astron. J.*, **67**, 256–266.

HOFFMANN, H. J., 1971. Entwicklung eines Detektors zur Massen und Geschwindigkeitsanalyse von kosmischen Staubteilchen, thesis, Univ. Heidelberg.

HÖRZ, F., HARTUNG, J. B., AND GAULT, D. E., 1971. Micrometeorite craters and related features on lunar rock surfaces, *Earth Planet. Sci. Letters*, **10**, 381–386.

INGHAM, M. F., 1961. Observations of the zodiacal light from a very high altitude station, *Mon. Not. Roy. Astron. Soc.*, **122**, 157–176.

JACCHIA, L. G., 1955. The physical theory of meteors, 8, fragmentation as cause of the faint meteor anomaly, *Astrophys. J.*, **121**, 521–527.

KEAYS, R. R., GANAPATHY, R., LAUL, J. C., ANDERS, E., HERZOG, G. F., AND JEFFERY, P. M., 1970. Trace elements and radioactivity in lunar rocks: implications for meteorite infall, solar wind flux, and formation conditions of Moon, *Science*, **167**, 490–493.

KIRSTEN, T., STEINBRUNN, F., AND ZÄHRINGER, J., 1971. Location and variation of trapped rare gases in Apollo 12 lunar samples, *Proc. Second Lunar Sci. Conf., Geochim. Cosmochim. Acta, Suppl.*, **2**, 2639–2652.

KORNBLUM, J. J., 1969. Concentration and collection of meteoric dust in the atmosphere, *J. Geophys. Res.*, **74**, 1908–1919.

LEINERT, C., 1971. The zodiacal light lines in the particle flux diagram, *Space Research XI*, 249–253.

LINDBLAD, B. A., ARINDER, G., AND WIESEL, T., 1970. Rocket observations of micrometeorites, *Space Research X*, 295–304.

MANDEVILLE, J. -C., AND VEDDER, J. F., 1971. Microcraters formed in glass by low density projectiles, *Earth Planet. Sci. Lett.*, **11**, 297–306.

NAUMANN, R. J., 1966. The near-earth meteoroid environment, *NASA Tech. Note* **D–3717**, Washington.

NAZAROVA, T. N., AND RYBAKOV, A. K., 1971. Meteor particle studies from space vehicles, *Space Research XI*, 357–361.

NEUKUM, G., 1971. thesis, Univ. Heidelberg.

NEUKUM, G., AND DIETZEL, H., 1971. On the development of the crater population on the Moon with time under meteoroid and solar wind bombardment, *Earth Planet. Sci. Lett.*, **12**, 59–66.

RAUSER, P., AND FECHTIG, H., 1972. Combined dust collection and detection experiment during a noctilucent cloud display above Kiruna, Sweden, *Space Research XII*, 391–402.

SHAPIRO, I. I., LAUTMAN, D. A., AND COLOMBO, G., 1966. The Earth's dust belt: fact or fiction? 1. Forces perturbing dust particle motion, *J. Geophys. Res.*, **71**, 5695–5704.

SHOEMAKER, E. M., BATSON, R. M., BEAN, A. L., CONRAD, C., JR., DAHLEM, D. H., GODDARD, E. N., HART, M. H., LARSON, K. B., SCHOBER, G. G., SCHLEICHER, D. L., SUTTON, R. L., SWANN, G. A., AND WATERS, A. C., 1970. Preliminary geologic investigation of the Apollo 12 landing site, Part A: geology of the Apollo 12 landing site, *Apollo 12 Preliminary Science Report, NASA*, **SP–235**.

SHOEMAKER, E. M., HAIT, M. H., SWANN, G. A., SCHLEICHER, D. L., DAHLEM, D. H., SCHOBER, G. G., AND SUTTON, R. C., 1970. Lunar regolith at tranquillity base, *Science*, **167**, 452–455.

SKRIVANEK, R. A., CARNEVALE, R. F., AND SARKISIAN, R. D., 1970. Results of in-flight shadowing performed on the ESRO rocket flight of 7 June 1968, *Space Research X*, 281–286.

VERNIANI, F., 1969. Structure and fragmentation of meteoroids, *Space Sci. Rev.*, **10**, 230–261.

WATSON, F. G., 1956. *Between the planets*, Harvard Univ. Press, Cambridge, Mass.

WEINBERG, J., 1964. The zodiacal light at 5300 Å, *Ann. d'Astrophys.*, **27**, 718–738.

YANIV, A., AND SHAFIR, U., 1967. Preliminary results of a micrometeoroid collection experiment in the Luster program, *Space Research VII*, 1403–1411.